Di- and Tritopic Poly(pyrazol-1-yl)borate Ligands: Synthesis, Characterization, and Reactivity toward [Mn(CO)$_5$Br]

Thorsten Morawitz,[†] Fan Zhang,[†] Michael Bolte,[†] Jan W. Bats,[‡] Hans-Wolfram Lerner,[†] and Matthias Wagner*,[†]

Institut für Anorganische Chemie, Goethe-Universität Frankfurt, Max-von-Laue-Strasse 7, D-60438 Frankfurt (Main), Germany, and Institut für Organische Chemie, Goethe-Universität Frankfurt, Max-von-Laue-Strasse 7, D-60438 Frankfurt (Main), Germany

Received June 2, 2008

Treatment of the ditopic phenylene-bridged bis(pyrazol-1-yl)borate K$_2$[*m*-C$_6$H$_4$(B(*t*Bu)pz$_2$)$_2$] (*m*-**1**) with [Mn(CO)$_5$Br] results in ligand degradation with formation of the pyrazabole-bridged macrocyclic dimer {*m*-C$_6$H$_4$(B(*t*Bu)pz)$_2$}$_2$ (**2**) and the triply pyrazolide-bridged dinuclear complex K[(OC)$_3$Mn(μ-pz)$_3$Mn(CO)$_3$] (**3**). Even though the Ph-substituted scorpionate ligands Li$_2$[*m*-C$_6$H$_4$(B(Ph)pz$_2$)$_2$] and Li$_2$[*p*-C$_6$H$_4$(B(Ph)pz$_2$)$_2$] (*m*-**5**, *p*-**5**) possess a significantly higher hydrolytic stability than *m*-**1**, their reaction with [Mn(CO)$_5$Br] also leads to B−N bond cleavage and gives the **3**-type complex Li[(OC)$_3$Mn(μ-pz)$_2$(μ-Br)Mn(CO)$_3$] (**6**). When, however, the corresponding tris(pyrazol-1-yl)borate ligands Li$_2$[*m*-C$_6$H$_4$(Bpz$_3$)$_2$] and Li$_2$[*p*-C$_6$H$_4$(Bpz$_3$)$_2$] (*m*-**8**, *p*-**8**) are employed, the clean formation of dinuclear Mn(CO)$_3$ complexes Li$_2$[*m*-C$_6$H$_4$(Bpz$_3$Mn(CO)$_3$)$_2$] and Li$_2$[*p*-C$_6$H$_4$(Bpz$_3$Mn(CO)$_3$)$_2$] (*m*-**11**, *p*-**11**) is observed. The same is true for the novel tritopic scorpionate Li$_3$[1,3,5-C$_6$H$_3$(Bpz$_3$)$_3$] (**10**), which gives ready access to the trinuclear Mn(CO)$_3$ complex [1,3,5-C$_6$H$_3$(Bpz$_3$Mn(CO)$_3$)$_3$] (**12**).

Introduction

In the last years, ditopic[1] poly(pyrazol-1-yl)borate ("scorpionate"[2,3]) ligands have shown great potential for the preparation of coordination polymers,[4−6] multiple-decker sandwich complexes,[7−10] metallo-macrocycles,[11] dinuclear complexes with cooperating metal ions,[12−15] and metalloenzyme models.[16] The two ligating sites have been linked together by a direct B−B bond,[17−19] the 1,1′-ferrocenylene moiety,[20] and the *m*- or *p*-phenylene ring.[12] Using as an example a *p*-phenylene-bridged derivative, Figure 1 illustrates how complexes of chelating bis(pyrazol-1-yl)borates **I** (R = alkyl, aryl) are able to adopt a configuration in which both coordinated metal ions act simultaneously on the same substrate molecule L*. This structural motif is interesting in the context of homogeneous bimetallic catalysis.

In contrast to **I**, facially coordinating tris(pyrazol-1-yl)borates **II** are likely to hold the two metal centers at a well-defined distance from each other, which renders these types of ligands useful for the synthesis of coordination polymers.

Given this broad range of potential applications, both classes of ligands, **I** and **II**, merit further investigations into their relative stabilities and coordination behavior.

In previous studies, we had to recognize that **I**-type scorpionates bearing *tert*-butyl substituents R at their boron atoms

* Corresponding author. Fax: +49 69 798 29260. E-mail: Matthias.Wagner@chemie.uni-frankfurt.de.
† Institut für Anorganische Chemie.
‡ Institut für Organische Chemie.

(1) For oligotopic poly(pyrazol-1-yl)borate ligands with polymeric or dendritic backbones, see: (a) Qin, Y.; Cui, C.; Jäkle, F. *Macromolecules* **2008**, *41*, 2972–2974. (b) Casado, M. A.; Hack, V.; Camerano, J. A.; Ciriano, M. A.; Tejel, C.; Oro, L. A. *Inorg. Chem.* **2005**, *44*, 9122–9124. For ditopic poly(pyrazol-1-yl)methane ligands, see: (c) Reger, D. L.; Gardinier, J. R.; Smith, M. D. *Polyhedron* **2004**, *23*, 291–299. (d) Reger, D. L.; Gardinier, J. R.; Grattan, T. C.; Smith, M. D. *J. Organomet. Chem.* **2005**, *690*, 1901–1912. (e) Reger, D. L.; Watson, R. P.; Smith, M. D.; Pellechia, P. J. *Organometallics* **2005**, *24*, 1544–1555. (f) Reger, D. L.; Watson, R. P.; Smith, M. D. *Inorg. Chem.* **2006**, *45*, 10077–10087. (g) Reger, D. L.; Watson, R. P.; Gardinier, J. R.; Smith, M. D.; Pellechia, P. J. *Inorg. Chem.* **2006**, *45*, 10088–10097.

(2) Trofimenko, S. *Chem. Rev.* **1993**, *93*, 943–980.

(3) Trofimenko, S. *Scorpionates−The Coordination Chemistry of Polypyrazolylborate Ligands*; Imperial College Press: London, 1999.

(4) Fabrizi de Biani, F.; Jäkle, F.; Spiegler, M.; Wagner, M.; Zanello, P. *Inorg. Chem.* **1997**, *36*, 2103–2111.

(5) Guo, S. L.; Peters, F.; Fabrizi de Biani, F.; Bats, J. W.; Herdtweck, E.; Zanello, P.; Wagner, M. *Inorg. Chem.* **2001**, *40*, 4928–4936.

(6) Morawitz, T.; Bolte, M.; Lerner, H.-W.; Wagner, M. *Z. Anorg. Allg. Chem.* **2008**, *634*, 1409–1414.

(7) Scholz, S.; Green, J. C.; Lerner, H.-W.; Bolte, M.; Wagner, M. *Chem. Commun.* **2002**, 36–37.

(8) Haghiri Ilkhechi, A.; Scheibitz, M.; Bolte, M.; Lerner, H.-W.; Wagner, M. *Polyhedron* **2004**, *23*, 2597–2604.

(9) Haghiri Ilkhechi, A.; Bolte, M.; Lerner, H.-W.; Wagner, M. *J. Organomet. Chem.* **2005**, *690*, 1971–1977.

(10) Haghiri Ilkhechi, A.; Mercero, J. M.; Silanes, I.; Bolte, M.; Scheibitz, M.; Lerner, H.-W.; Ugalde, J. M.; Wagner, M. *J. Am. Chem. Soc.* **2005**, *127*, 10656–10666.

(11) Zhang, F.; Morawitz, T.; Bieller, S.; Bolte, M.; Lerner, H.-W.; Wagner, M. *Dalton Trans.* **2007**, 4594–4598.

(12) Bieller, S.; Zhang, F.; Bolte, M.; Bats, J. W.; Lerner, H.-W.; Wagner, M. *Organometallics* **2004**, *23*, 2107–2113.

(13) Bieller, S.; Bolte, M.; Lerner, H.-W.; Wagner, M. *Inorg. Chem.* **2005**, *44*, 9489–9496.

(14) Zhang, F.; Bolte, M.; Lerner, H.-W.; Wagner, M. *Organometallics* **2004**, *23*, 5075–5080.

(15) Morawitz, T.; Bolte, M.; Lerner, H.-W.; Wagner, M. *Z. Anorg. Allg. Chem.* **2008**, *634*, 1570–1574.

(16) Ruth, K.; Tüllmann, S.; Vitze, H.; Bolte, M.; Lerner, H.-W.; Holthausen, M. C.; Wagner, M. *Chem.−Eur. J.* **2008**, *14*, 6754–6770.

(17) Brock, C. P.; Das, M. K.; Minton, R. P.; Niedenzu, K. *J. Am. Chem. Soc.* **1988**, *110*, 817–822.

(18) Harden, N. C.; Jeffery, J. C.; McCleverty, J. A.; Rees, L. H.; Ward, M. D. *New J. Chem.* **1998**, *22*, 661–663.

(19) Armaroli, N.; Accorsi, G.; Barigelletti, F.; Couchman, S. M.; Fleming, J. S.; Harden, N. C.; Jeffery, J. C.; Mann, K. L. V.; McCleverty, J. A.; Rees, L. H.; Starling, S. R.; Ward, M. D. *Inorg. Chem.* **1999**, *38*, 5769–5776.

(20) Jäkle, F.; Polborn, K.; Wagner, M. *Chem. Ber.* **1996**, *129*, 603–606.

10.1021/om800504r CCC: $40.75
Publication on Web 09/10/2008

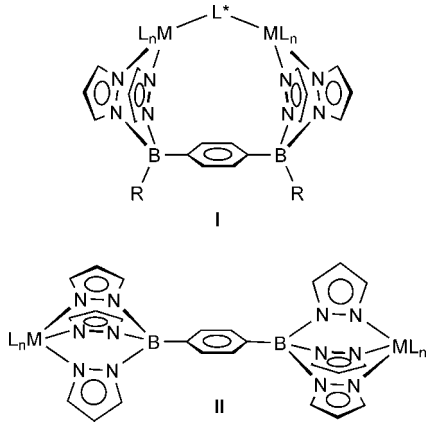

Figure 1. Different binding modes of ditopic bis- (**I**) and tris(pyrazol-1-yl)borate ligands (**II**).

Scheme 1. Reaction of the Ditopic Bis(pyrazol-1-yl)borate *m*-1 with [Mn(CO)$_5$Br][a]

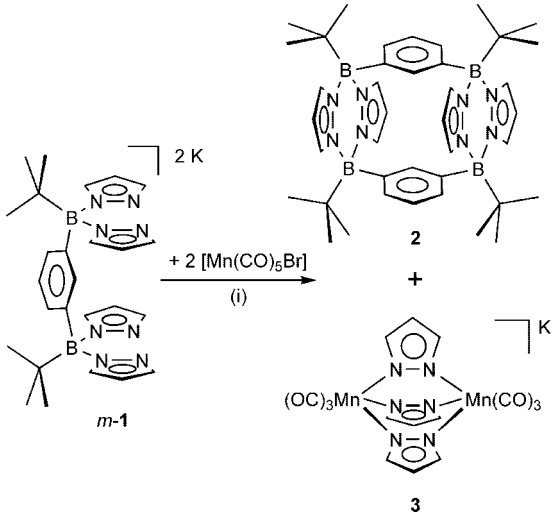

[a] Conditions: (i) THF, rt.

are prone to B−N bond cleavage and loss of pyrazolyl substituents, both during hydrolytic[11,12] and nonhydrolytic[21] processes. Replacement of the *tert*-butyl groups by more electronegative and less sterically demanding C_6F_5 substituents results in a greatly enhanced hydrolytic stability of the ligand framework, but also in fundamentally different solid state structures of related complexes.[6] We now report on the phenyl derivatives *m*-**5**/*p*-**5** (Scheme 2), the **II**-type tris(pyrazol-1-yl)-borates *m*-**8**/*p*-**8** (Scheme 3), and on the first *tri*topic tris(pyrazol-1-yl)borate **10** (Scheme 3), which is a promising building block for the generation of two-dimensional transition metal aggregates. The sensitivity of the new compounds toward air and moisture will be assessed first. After that, we will compare the reactions of *m*-**5**/*p*-**5**, *m*-**8**/*p*-**8**, **10**, and the previously prepared *tert*-butyl derivative *m*-**1**[12] (Scheme 1) with [Mn(CO)$_5$Br] under strictly anhydrous conditions.

Results and Discussion

Synthesis. Reaction of the aminoboranes *m*-**4**[22]/*p*-**4**[15] with 2 equiv of lithium pyrazolide (Lipz) and 2 equiv of pyrazole (Hpz)

Scheme 2. Synthesis of the Ditopic Bis(pyrazol-1-yl)borate Ligands *m*-5 and *p*-5; Reaction of *m*-5 and *p*-5 with [Mn(CO)$_5$Br][a]

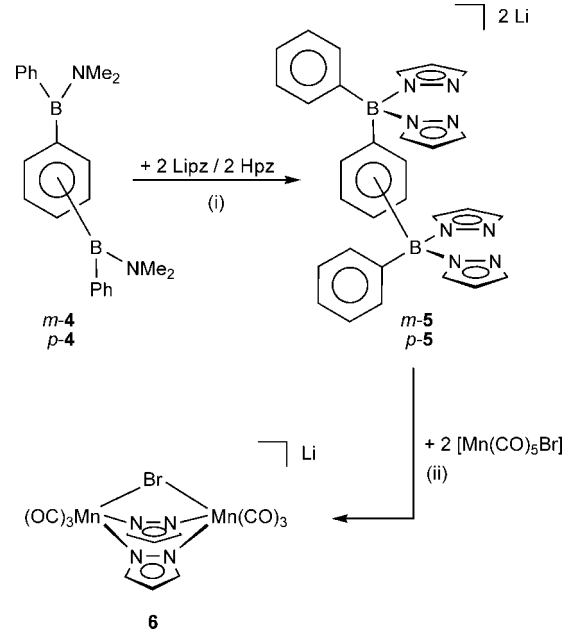

[a] Conditions: (i) toluene, reflux; (ii) THF, rt.

in refluxing toluene gave the phenyl-substituted scorpionates *m*-**5** and *p*-**5** in high yield via a transamination reaction (Scheme 2). Similarly, *m*-**8**/*p*-**8** were accessible from *m*-**7**/*p*-**7**,[22] 2 equiv of Lipz, and 4 equiv of Hpz (Scheme 3). In the case of the tritopic scorpionate, 3 equiv of Lipz and 6 equiv of Hpz were required for the almost quantitative transformation of **9**[22] into **10** (Scheme 3).

To test the hydrolytic stability of *m*-**5**/*p*-**5**, both compounds were dissolved in THF and stirred under air at rt. After 12 h, their ^{1}H NMR spectra still showed no signs of decomposition; after 36 h, however, a significant amount of free pyrazole was present in the solution (the integral ratios of the resonances of the pyrazole and pyrazolyl protons amounted to Hpz:*m*-**5** ≈ Hpz:*p*-**5** = 1:2). *m*-**5**/*p*-**5** are thus much less sensitive toward air and moisture than the corresponding *tert*-butyl derivatives. In the latter compounds, the B−N bonds are cleaved to a degree of about 50% already after 30 min under the same conditions. The tris(pyrazol-1-yl)borates *m*-**8**/*p*-**8** could be stirred for 24 h in wet MeOH without hydrolysis.

Treatment of *m*-**1** with 2 equiv of [Mn(CO)$_5$Br] in THF did not give the expected dinuclear Mn(CO)$_4$ complex with η^2-coordinating bis(pyrazol-1-yl)borate moieties even though the compound [(2,2′-bipyridyl)Mn(CO)$_4$]SO$_3$CF$_3$, which shows a similar structural motif to our target molecule, has been described.[23] Instead, we isolated two reaction products: (i) the macrocyclic pyrazabole **2** in a yield of almost 30% and (ii) the triply pyrazolide-bridged dinuclear manganese tricarbonyl complex **3** (Scheme 1). The metal-induced elimination of pyrazolide from poly(pyrazol-1-yl)borate ligands with subsequent dimerization of the resulting (pyrazol-1-yl)borane is not without precedent. For example, *ansa*-ferrocenes with pyrazabole

(21) Bieller, S.; Haghiri, A.; Bolte, M.; Bats, J. W.; Wagner, M.; Lerner, H.-W. *Inorg. Chim. Acta* **2006**, *359*, 1559–1572.

(22) See the Supporting Information of this publication for the synthesis and characterization of these compounds.

(23) Scheiring, T.; Kaim, W.; Fiedler, J. *J. Organomet. Chem.* **2000**, *598*, 136–141, for a recent review on chemistry surrounding group 7 complexes that possess poly(pyrazol-1-yl)borate ligands, see: Lail, M.; Pittard, K. A.; Gunnoe, T. B. *Adv. Organomet. Chem.* **2008**, *56*, 95–153.

Scheme 3. Synthesis of the Ditopic Tris(pyrazol-1-yl)borates *m*-8 and *p*-8 and of the Tritopic Ligand 10[a]

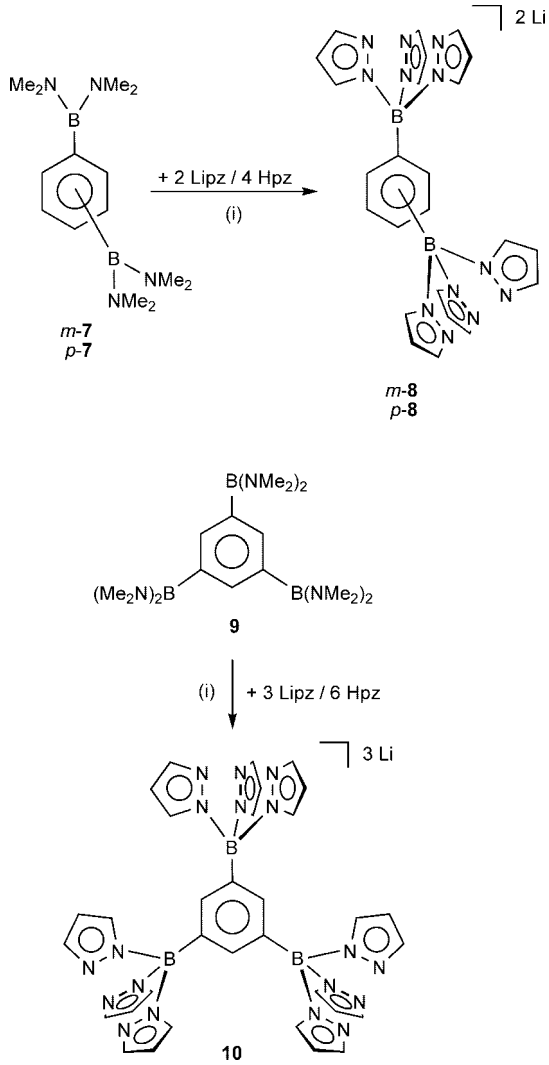

[a] Conditions: (i) toluene, reflux.

Scheme 4. Synthesis of the Di- and Trinuclear $Mn(CO)_3$ Complexes *m*-11, *p*-11, and 12[a]

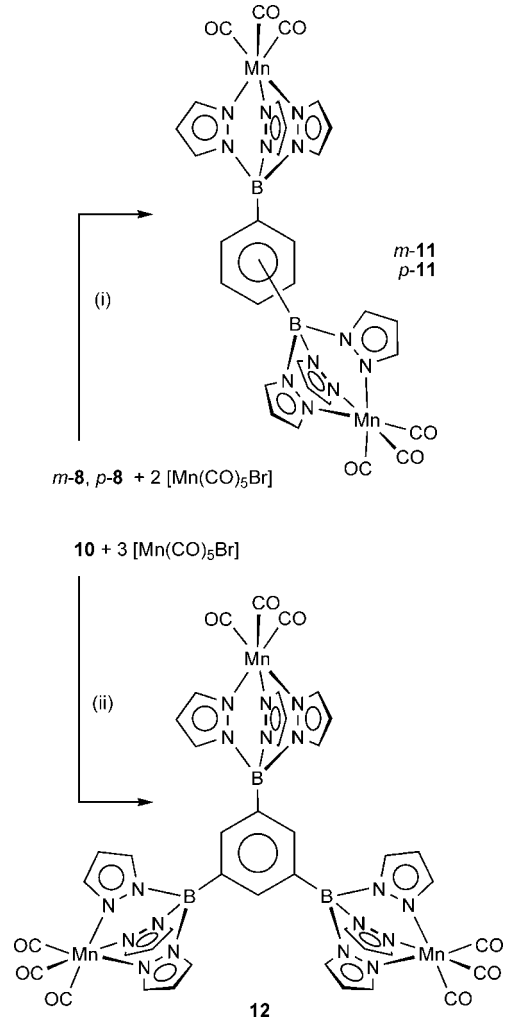

[a] Conditions: (i) THF, rt; (ii) toluene, rt.

bridges[24−26] have been obtained upon reaction of [1,1′-fc$(Bpz_3)_2$]$^{2-}$ with $ZrCl_4$ or $ZrCl_4(THF)_2$ (fc = $(C_5H_4)_2Fe$).[4]

In order to find out whether phenyl substituents in the position of the *tert*-butyl groups would help to suppress B−N bond cleavage (as it was the case in the reaction with water), we also treated *m*-**5** with $[Mn(CO)_5Br]$. A complex mixture of compounds formed, and *in situ* NMR spectroscopy indicated major degradation of the ligand system. The only reaction product that could be isolated in pure form was the dinuclear Mn^I complex **6** (Scheme 2), which is formally derived from **3** (Scheme 1) by substitution of bromide for one of the bridging pyrazolide ions.

To test whether the connectivity pattern at the central bridging unit has any significant influence on the course of the reaction, the experiment was repeated with *p*-**5** and $[Mn(CO)_5Br]$. However, we obtained similar results and again observed the formation of substantial amounts of **6**.

In contrast to the bis(pyrazol-1-yl)borate ligands *m*-**1**, *m*-**5**, and *p*-**5**, the corresponding di- and tritopic tris(pyrazol-1-yl)borate ligands *m*-**8**, *p*-**8**, and **10** gave the aimed-for $Mn(CO)_3$ complexes cleanly and in excellent yields (Scheme 4).

Spectroscopic Characterization. Each of the bis(pyrazol-1-yl)borates *m*-**5** and *p*-**5** shows one ^{11}B NMR resonance[27] with a chemical shift value typical of four-coordinate boron nuclei (*m*-**5**: 2.0 ppm, *p*-**5**: 1.7 ppm). In both molecules, the two phenyl groups on one hand and the four pyrazolyl rings on the other give rise to only one set of signals in the ^1H as well as the ^{13}C NMR spectrum. The nuclei of the bridging unit of *m*-**5** resonate at $\delta(^1H)/\delta(^{13}C)$ = 6.50/133.7 (H/C-4,6), 6.80/126.1 (H/C-5), and 7.31/142.4 (H/C-2), while the phenylene linker in *p*-**5** gives rise to signals at $\delta(^1H)/\delta(^{13}C)$ = 6.82/134.3. The proton integral values indicate a 2:5:6 ratio for the bridging element, the phenyl group, and the pyrazolyl group both in *m*-**5** and in *p*-**5**. All NMR data are therefore in accord with the proposed composition and symmetry of the ligand frameworks (Scheme 2).

The ^{11}B NMR signals[27] of the three tris(pyrazol-1-yl)borates testify to the presence of four-coordinate boron nuclei (*m*-**8**: 1.9 ppm, *p*-**8**: 2.2 ppm, **10**: 2.3 ppm). According to their ^1H and ^{13}C NMR spectra, *m*-**8**, *p*-**8**, and **10** possess six, six, and nine magnetically equivalent pyrazolyl rings, respectively. The

(24) Jäkle, F.; Priermeier, T.; Wagner, M. *J. Chem. Soc., Chem. Commun.* **1995**, 1765–1766.

(25) Jäkle, F.; Priermeier, T.; Wagner, M. *Organometallics* **1996**, *15*, 2033–2040.

(26) Herdtweck, E.; Jäkle, F.; Opromolla, G.; Spiegler, M.; Wagner, M.; Zanello, P. *Organometallics* **1996**, *15*, 5524–5535.

(27) Nöth, H.; Wrackmeyer, B. Nuclear Magnetic Resonance Spectroscopy of Boron Compounds. In *NMR Basic Principles and Progress*; Diehl, P.; Fluck, E.; Kosfeld, R., Eds.; Springer: Berlin, 1978.

phenylene ^{13}C resonances of *m*-**8**/*p*-**8** are very similar to those of their bis(pyrazol-1-yl)borate relatives *m*-**5**/*p*-**5**. In the proton NMR spectra we find major differences for the chemical shift values of H-2 (*m*-**8**: 6.79 ppm vs *m*-**5**: 7.31 ppm) and *p*-C_6H_4 (*p*-**8**: 6.49 ppm vs *p*-**5**: 6.82 ppm). The resonances of the C_6H_3 spacer in **10** appear at $\delta(^1H) = 6.45$ and $\delta(^{13}C) = 139.8$.

The ^1H NMR spectrum of **2** contains only one *tert*-butyl signal, one set of signals for the *m*-phenylene ring, and one set of resonances for the pyrazolyl groups. The same is true for the ^{13}C NMR spectrum. This leads to the conclusion that the molecular framework of **2** possesses high symmetry on the NMR time scale. Most importantly, we find only one $^1H/^{13}C$ resonance for pzH/C-3,5. This observation, together with an ^{11}B NMR signal in the shift range of four-coordinate boron, provides evidence for the presence of pyrazabole moieties in compound **2**. The NMR shifts of **3** and its CO stretching frequencies are in accord with the corresponding published data of $(Et_4N)[(OC)_3Mn(\mu\text{-pz})_3Mn(CO)_3]$ ($\tilde{\nu}$(CO) = 2016, 1917 cm^{-1}).[28] Interestingly, we observe very similar CO bands in the bromide-bridged complex **6** ($\tilde{\nu}$(CO) = 2017 (s), 1930 (s), 1904 (shoulder) cm^{-1}), thus reflecting a comparable degree of Mn−CO back-bonding in both compounds.

Complexation of *m*-**8** and *p*-**8** with $Mn(CO)_3$ fragments results in a shift of all ligand resonances to lower field. Particularly pronounced deshielding is observed for H-2/H-4,6 in *m*-**11** (8.50/8.14 ppm vs 6.79/6.37 ppm in *m*-**8**) and *p*-C_6H_4 in *p*-**11** (8.16 ppm vs 6.49 ppm in *p*-**8**). In the ^{13}C NMR spectra, the largest downfield shift occurs for one of the pzC-3,5 signals, which appears at 145.9 ppm both in *m*-**11** and in *p*-**11**.

For solubility reasons, the NMR spectra of the free tritopic scorpionate **10** and its $Mn(CO)_3$ complex **12** had to be recorded in different solvents. Nevertheless, the same qualitative trends are apparent as in the cases of the ditopic congeners.

The frequencies of the carbonyl stretching vibrations in the infrared spectra of *m*-**11**, *p*-**11**, and **12** lie in the same range as those of the related mononuclear complex $[HBpz_3Mn(CO)_3]$[29] and thus do not merit further discussion.

X-ray Crystal Structure Determination. Crystal data and structure refinement details for **2**, **3**(Et_2O), *m*-**11**, and **12** are compiled in Tables 1 and 2; for crystal structure analyses of *p*-**5**(12-c-4)$_2$, **6**$(THF)_4$, *m*-**7**, *p*-**7**, **9**, and *p*-**11** see the Supporting Information of this publication.

Compound **2** possesses a centrosymmetric macrocyclic structure composed of two pyrazabole moieties that are connected to each other by two *m*-phenylene linkers (Figure 2). The B_2N_4 ring does not adopt a boat conformation as in other bridged pyrazabole derivatives,[24−26,30,31] but is considerably twisted. B(1) and B(2) deviate by 0.55 and 0.31 Å, respectively, in opposite directions from the plane of the pyrazolyl group pz[N(1)], and they deviate by 0.27 and 0.48 Å, also in opposite directions, from the plane of the pyrazolyl group pz[N(3)]. The B−N bond lengths are not equal but fall in the range between B(2)−N(2) = 1.576(2) Å and B(1)−N(1) = 1.611(2) Å (cf. B−N bond length range in $Ph_2B(\mu\text{-pz})_2BPh_2$: 1.568(4)−1.590(4) Å[32]). Twisting of the pyrazabole unit as well as B−N bond elongation in **2** is apparently the result of intramolecular steric congestion between the pyrazole and *m*-phenylene rings. The *m*-phenylene ring itself is planar, but the boron substituents deviate from this plane by 0.25 Å (B(1)) and 0.19 Å (B(2$^{\#}$)) into the same direction.

The second product of the $[Mn(CO)_5Br]$-induced degradation reaction of *m*-**1**, $K[(OC)_3Mn(\mu\text{-pz})_3Mn(CO)_3]$, crystallizes from Et_2O/hexane as diethyl ether adduct **3**(Et_2O) and forms contact ion pairs in the solid state (Figure 3). The asymmetric unit of the crystal consists of (i) two dinuclear Mn^I complexes, (ii) one

Table 1. Selected Crystallographic Data of the Compounds 2 and 3(Et_2O)

	2	**3**(Et_2O)
formula	$C_{40}H_{56}B_4N_8$	$C_{38}H_{38}K_2Mn_4N_{12}O_{14}$
fw	692.17	1184.76
color, shape	colorless, block	yellow, block
temp (K)	149(2)	173(2)
radiation	Mo Kα 0.71073 Å	Mo Kα, 0.71073 Å
cryst syst	monoclinic	monoclinic
space group	$P2_1/c$	$P2_1/n$
a (Å)	11.585(2)	10.3347(11)
b (Å)	11.753(3)	16.2699(12)
c (Å)	14.228(2)	29.092(3)
α (deg)	90	90
β (deg)	92.957(11)	91.446(9)
γ (deg)	90	90
V (Å^3)	1934.7(7)	4890.1(8)
Z	2	4
D_{calcd} (g cm^{-3})	1.188	1.609
F(000)	744	2400
μ (mm^{-1})	0.070	1.254
cryst size (mm^3)	0.30 × 0.20 × 0.10	0.24 × 0.21 × 0.13
no of rflns collected	24 569	39 572
no of indep rflns (R_{int})	5710 (0.0638)	8589 (0.0895)
no. of data/restraints/params	5710/0/266	8589/0/631
GOOF on F^2	1.070	0.582
R1, wR2 ($I > 2\sigma(I)$)	0.0563, 0.1049	0.0400, 0.0552
R1, wR2 (all data)	0.1141, 0.1224	0.1126, 0.0651
largest diff peak and hole (e Å^{-3})	0.349, −0.266	0.496, −0.247

Table 2. Crystallographic Data of the Compounds *m*-11 and 12

	m-**11**	**12**
formula	$C_{30}H_{22}B_2Mn_2N_{12}O_6 \cdot CH_2Cl_2$	$C_{42}H_{30}B_3Mn_3N_{18}O_9 \cdot 4C_4H_8O$
fw	863.02	1416.51
color, shape	light yellow, block	yellow, block
temp (K)	173(2)	173(2)
radiation	Mo Kα, 0.71073 Å	MoK, 0.71073 Å
cryst syst	monoclinic	triclinic
space group	$P2_1/n$	$P\bar{1}$
a (Å)	15.5531(6)	10.1742(6)
b (Å)	14.6474(5)	17.0682(10)
c (Å)	16.5291(6)	19.9745(12)
α (deg)	90	83.934(5)
β (deg)	103.423(3)	89.307(5)
γ (deg)	90	83.283(5)
V (Å^3)	3662.7(2)	3425.6(4)
Z	4	2
D_{calcd} (g cm^-)	1.565	1.373
F(000)	1744	1460
μ (mm^{-1})	0.897	0.617
cryst size (mm)	0.38 × 0.35 × 0.32	0.22 × 0.19 × 0.18
no of rflns collected	62 614	54 872
no of indep rflns (R_{int})	10 254 (0.0408)	12 519 (0.0799)
no. of data/restraints/params	10 254/0/524	12 519/26/831
GOOF on F^2	1.030	1.035
R1, wR2 ($I > 2\sigma(I)$)	0.0335, 0.0862	0.0709, 0.1916
R1, wR2 (all data)	0.0365,0.0881	0.1054, 0.2105
largest diff peak and hole (e Å^{-3})	0.367, −0.569	2.048,−0.676

(28) Trofimenko, S. *J. Am. Chem. Soc.* **1969**, *91*, 5410–5411.
(29) Joachim, J. E.; Apostolidis, C.; Kanellakopulos, B.; Maier, R.; Marques, N.; Meyer, D.; Müller, J.; Matos, A. P. d.; Nuber, B.; Rebizant, J.; Ziegler, M. L. *J. Organomet. Chem.* **1993**, *448*, 119–129.
(30) Hsu, L.-Y.; Mariategui, J. F.; Niedenzu, K.; Shore, S. G. *Inorg. Chem.* **1987**, *26*, 143–147.
(31) Das, M. K.; Niedenzu, K.; Nöth, H. *Inorg. Chem.* **1988**, *27*, 1112–1114.
(32) Atwood, V. O.; Atwood, D. A.; Cowley, A. H.; Trofimenko, S. *Polyhedron* **1992**, *11*, 711–713.

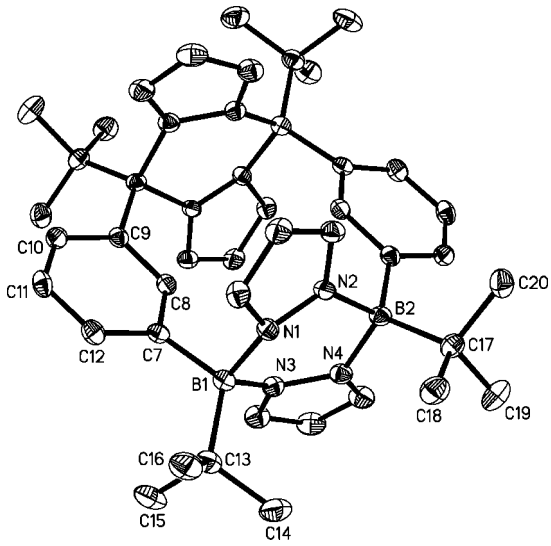

Figure 2. Structure of **2** in the crystal. Displacement ellipsoids are drawn at the 50% probability level; hydrogen atoms are omitted for clarity. Selected bond lengths (Å), bond angles (deg), and torsion angles (deg): B(1)−N(1) = 1.611(2), B(1)−N(3) = 1.582(2), B(2)−N(2) = 1.576(2), B(2) −N(4) = 1.601(2), B(1)−C(7) = 1.626(2), B(2)−C(9#) = 1.633(2), B(1)−C(13) = 1.662(2), B(2)−C(17) = 1.665(2); N(1)−B(1)−N(3) = 103.7(1), N(2)−B(2)−N(4) = 103.8(1), C(13)−B(1)−C(7) = 118.2(1), C(17)−B(2)−C(9#) = 117.8(1); C(8)−C(7)−B(1)−C(13) = −153.8(1), C(8#)−C(9#)−B(2)−C(17) = −149.0(1). Symmetry transformations used to generate equivalent atoms: $-x+1,-y+1, -z$ (#).

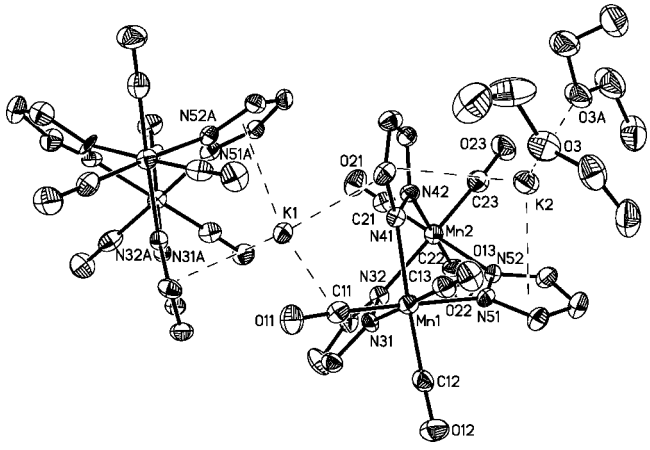

Figure 3. Structure of **3**(Et_2O) in the crystal. Displacement ellipsoids are drawn at the 50% probability level; hydrogen atoms are omitted for clarity. Selected bond lengths (Å) and bond angles (deg): Mn(1)−N(31) = 2.042(4), Mn(1)−N(41) = 2.074(4), Mn(1)−N(51) = 2.080(4), Mn(2)−N(32) = 2.066(4), Mn(2)−N(42) = 2.070(4), Mn(2)−N(52) = 2.072(4); N(31)−Mn(1)−N(41) = 88.7(2), N(31)−Mn(1)−N(51) = 88.4(2), N(41)−Mn(1)−N(51) = 87.0(2), N(32)−Mn(2)−N(42) = 89.1(2), N(32)−Mn(2)−N(52) = 88.7(2), N(42)−Mn(2)−N(52) = 85.8(2). Mn(1A)−N(31A) = 2.050(4), Mn(1A)−N(41A) = 2.121(5), Mn(1A)−N(51A) = 2.045(4), Mn(2A)−N(32A) = 2.064(3), Mn(2A)−N(42A) = 2.128(5), Mn(2A)−N(52A) = 2.051(4); N(31A)−Mn(1A)−N(41A) = 88.7(2), N(31A)−Mn(1A)−N(51A) = 86.7(2), N(41A)−Mn(1A)−N(51A) = 88.0(2), N(32A)−Mn(2A)−N(42A) = 88.7(2), N(32A)−Mn(2A)−N(52A) = 86.2(2), N(42A)−Mn(2A)−N(52A) = 87.3(2).

K^+ ion occupying a bridging position between them (K(1)), and (iii) a second K^+ ion located at a terminal position (K(2)). K(1) is surrounded by the π-faces of four pyrazole rings, whereas K(2) is involved in π-interactions with two pyrazolyl rings and

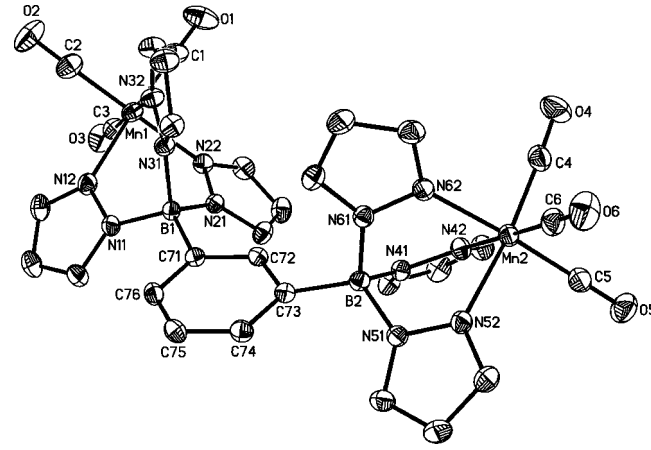

Figure 4. Structure of *m*-**11** in the crystal. Displacement ellipsoids are drawn at the 50% probability level; hydrogen atoms are omitted for clarity. Selected bond lengths (Å), bond angles (deg), and torsion angles (deg): Mn(1)−N(12) = 2.066(1), Mn(1)−N(22) = 2.053(1), Mn(1)−N(32) = 2.032(1), Mn(2)−N(42) = 2.054(1), Mn(2)−N(52) = 2.071(1), Mn(2)−N(62) = 2.027(1), Mn(1)−C(1) = 1.810(2), Mn(1)−C(2) = 1.810(2), Mn(1)−C(3) = 1.819(2), Mn(2)−C(4) = 1.810(2), Mn(2)−C(5) = 1.822(1), Mn(2)−C(6) = 1.810(2); N(12)−Mn(1)−N(22) = 85.8(1), N(12)−Mn(1)−N(32) = 85.9(1), N(22)−Mn(1)−N(32) = 84.6(1), N(42)−Mn(2)−N(52) = 85.9(1), N(42)−Mn(2)−N(62) = 85.8(1), N(52)−Mn(2)−N(62) = 84.6(1); C(72)−C(71)−B(1)−N(31) = −76.5(1), C(72)−C(73)−B(2)−N(61) = 77.6(1).

σ-bonded to two diethyl ether ligands. The distances between K(1) and the ring centroids (COG) of the pyrazolyl ligands amount to K(1)−COG(pz[N(31)]) = 3.016 Å, K(1)−COG(pz[N(41)]) = 3.371 Å, K(1)−COG(pz[N(31A)]) = 2.963 Å, and K(1)−COG(pz[N(51A)]) = 2.903 Å. In the case of K(2), we find distances of 2.987 and 2.930 Å to the centroids of pz[N(41)] and pz[N(51)], respectively.

The average Mn−N bond length of the two anions within the asymmetric unit of **3**(Et_2O) is 2.072(5) Å, and the average N−Mn−N bond angle is 87.8(2)°. We note that a targeted synthesis of the related complex $(Et_4N)[(OC)_3Mn(\mu\text{-pz})_3Mn(CO)_3]$ from $[Mn(CO)_5Br]$ and 1.5 equiv of pyrazolide ion has been described by Trofimenko.[28] The triethylammonium salt was characterized by X-ray powder crystallography and found to be isostructural with the complex $(Et_3NH)[(OC)_3Re(\mu\text{-pz})_3Mn(CO)_3]$, for which a single crystal structure analysis exists.[33]

In line with the NMR spectra of *m*-**11**, X-ray crystallography provides conclusive evidence for the successful preparation of the targeted dinuclear $Mn(CO)_3$ complex with two facially coordinating tris(pyrazol-1-yl)borate moieties (Figure 4).

The molecule possesses C_1 symmetry in the solid state, but the molecular framework closely approaches C_s symmetry with the mirror plane running perpendicular to the bridging six-membered ring through the carbon atoms C(72) and C(75). One pyrazolyl ring of each scorpionate moiety is located in a position almost orthogonal to the phenylene spacer (dihedral angles: 80.6° for pz[N(31)], 84.6° for pz[N(61)]). Somewhat surprisingly, both these rings occupy space at the same side of the bridging element, which leads to a short distance between H(35)/H(65) of 2.368 Å and to an even closer contact between H(25)/H(45) of 2.147 Å. Most likely as a result of steric repulsion between H(25) and H(45), the boron atoms are displaced out

(33) Ardizzoia, G. A.; LaMonica, G.; Maspero, A.; Moret, M.; Masciocchi, N. *Eur. J. Inorg. Chem.* **2000**, *18*, 1–187.

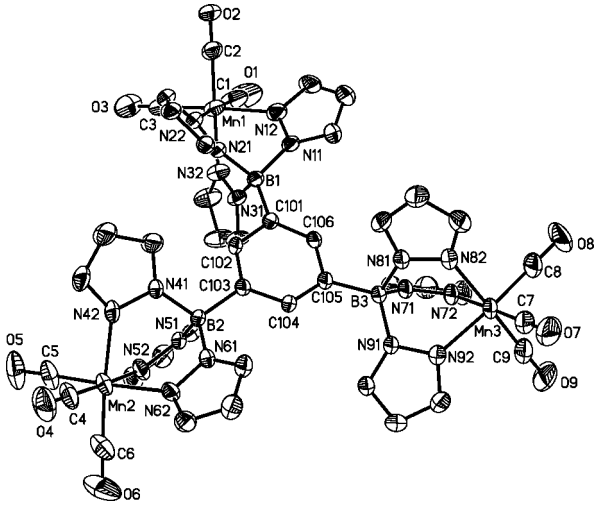

Figure 5. Structure of **12** in the crystal. Displacement ellipsoids are drawn at the 50% probability level; hydrogen atoms are omitted for clarity. Selected bond lengths (Å), bond angles (deg), and torsion angles (deg): Mn(1)−N(12) = 2.070(4), Mn(1)−N(22) = 2.060(4), Mn(1)−N(32) = 2.020(4), Mn(2)−N(42) = 2.065(4), Mn(2)−N(52) = 2.024(4), Mn(2)−N(62) = 2.060(4), Mn(3)−N(72) = 2.052(5), Mn(3)−N(82) = 2.026(4), Mn(3)−N(92) = 2.056(4), Mn(1)−C(1) = 1.799(6), Mn(1)−C(2) = 1.796(5), Mn(1)−C(3) = 1.806(6), Mn(2)−C(4) = 1.818(6), Mn(2)−C(5) = 1.802(6), Mn(2)−C(6) = 1.799(6), Mn(3)−C(7) = 1.804(7), Mn(3)−C(8) = 1.800(6), Mn(3)−C(9) = 1.817(6); N(12)−Mn(1)−N(22) = 85.0(2), N(12)−Mn(1)−N(32) = 85.7(2), N(22)−Mn(1)−N(32) = 85.8(1), N(42)−Mn(2)−N(52) = 85.2(2), N(42)−Mn(2)−N(62) = 85.3(1), N(52)−Mn(2)−N(62) = 86.2(2), N(72)−Mn(3)−N(82) = 85.4(2), N(72)−Mn(3)−N(92) = 84.9(2), N(82)−Mn(3)−N(92) = 85.7(2); C(102)−C(101)−B(1)−N(31) = −76.6(5), C(102)−C(103)−B(2)−N(51) = 74.9(4), C(104)−C(105)−B(3)−N(81) = −99.3(5).

of the plane of the *m*-phenylene ring by 0.197 Å (B(1)) and 0.237 Å (B(2)). The average Mn−N bond lengths amount to 2.051(1) Å but are spread over an interval from 2.032(1) Å/2.027(1) Å for the related bonds Mn(1)−N(32)/Mn(2)−N(62) to 2.066(1) Å/2.071(1) Å for Mn(1)−N(12)/Mn(2)−N(52); in the parent compound [$HBpz_3Mn(CO)_3$], the three Mn−N bonds have the same length of 2.177(8) Å,[29] whereas in the complex [$(pzBpz_3)Mn(CO)_3$], the average Mn−N bond length is 2.048(3) Å.[34] All bond angles about the Mn^I ions in *m*-**11** deviate by less than 7° from the ideal values of 90° and 180°.

The trinuclear $Mn(CO)_3$ complex **12** (C_1 symmetry in the crystal lattice; Figure 5) contains one fragment, consisting of the scorpionate moiety at B(1), the phenylene linker, and the scorpionate unit at B(2), which closely resembles *m*-**11**: Two pyrazolyl rings, pz[N(31)] and pz[N(51)], are roughly orthogonal to the phenylene linker and positioned at the same side of it. This conformation again results in short intramolecular contacts between pyrazolyl rings (H(23)···H(45) = 2.229 Å; H(35)···H(55) = 2.232 Å). Concomitantly, B(1) and B(2) are bent by 0.138 and 0.230 Å, respectively, in the same direction out of the phenylene plane. In the third scorpionate fragment, the orthogonal pyrazolyl substituent pz[N(81)] resides at the opposite side of the C_6H_3 linker; the boron atom B(3) shows a corresponding displacement of 0.240 Å. Bond lengths and angles in **12** reach similar values to those in *m*-**11**.

(34) MacNeil, J. H.; Roszak, A. W.; Baird, M. C.; Preston, K. F.; Rheingold, A. L. *Organometallics* **1993**, *12*, 4402–4412.

Conclusion

The *tert*-butyl-substituted bis(pyrazol-1-yl)borate ligand $K_2[m\text{-}C_6H_4(B(t\text{Bu})pz_2)_2]$ (*m*-**1**) is highly prone to hydrolysis of its B−N bonds. This leads to the conclusion that the bulky substituent at boron does not primarily effect a kinetic stabilization of the (pyrazol-1-yl)borate fragment, but rather promotes the liberation of pyrazole, most likely because there is less steric crowding in the resulting three-coordinate borane. In line with that, we observe a greatly enhanced hydrolytic stability of the corresponding scorpionates $Li_2[m\text{-}C_6H_4(B(Ph)pz_2)_2]$ and $Li_2[p\text{-}C_6H_4(B(Ph)pz_2)_2]$ (*m*-**5**, *p*-**5**), which bear less sterically demanding and more electronegative phenyl substituents at their boron atoms.

In contrast to the pronounced differences in the reactivity toward water of *m*-**1** on one hand and *m*-**5**/*p*-**5** on the other, the behavior of these three ligands toward $[Mn(CO)_5Br]$ appears to be rather similar. In none of the three cases have we been able to isolate complexes of the form $[RB(t\text{Bu,Ph})pz_2Mn(CO)_4]$, but rather obtained pyrazolide-bridged dinuclear Mn^I complexes $K[(OC)_3Mn(\mu\text{-}pz)_3Mn(CO)_3]$ (**3**; from *m*-**1**) and $Li[(OC)_3Mn(\mu\text{-}pz)_2(\mu\text{-}Br)Mn(CO)_3]$ (**6**; from *m*-**5**, *p*-**5**).

Under similar reaction conditions, the related tris(pyrazol-1-yl)borate ligands $Li_2[m\text{-}C_6H_4(Bpz_3)_2]$ and $Li_2[p\text{-}C_6H_4(Bpz_3)_2]$ (*m*-**8**, *p*-**8**) give the corresponding dinuclear $Mn(CO)_3$ complexes $Li_2[m\text{-}C_6H_4(Bpz_3Mn(CO)_3)_2]$ and $Li_2[p\text{-}C_6H_4(Bpz_3Mn(CO)_3)_2]$ (*m*-**11**, *p*-**11**) in high yields. Since the steric demand of the phenyl and pyrazolyl ring is roughly the same, the greater stability of *m*-**8** and *p*-**8** is most likely due to the presence of the additional donor sites, which finally lead to a face-capping coordination mode in *m*-**11** and *p*-**11**.

We synthesized the novel tritopic scorpionate $Li_3[1,3,5\text{-}C_6H_3(Bpz_3)_3]$ (**10**) along with the trinuclear $Mn(CO)_3$ complex $[1,3,5\text{-}C_6H_3(Bpz_3Mn(CO)_3)_3]$ (**12**). We are currently investigating the potential of **10** for the preparation of two-dimensional transition metal aggregates and metal-organic frameworks.

Experimental Section

General Remarks. All reactions and manipulations of air-sensitive compounds were carried out in dry, oxygen-free argon using standard Schlenk ware. CH_2Cl_2 was passed through a 4 Å molecular sieves column prior to use. All other solvents were freshly distilled under argon from Na/benzophenone. IR: Jasco FT-IR 4200 spectrometer. NMR: Bruker AMX 250, AMX 300, AMX 400, Bruker DPX 250. Chemical shifts are referenced to residual solvent signals (^1H, $^{13}C\{^1H\}$) or external $BF_3 \times Et_2O$ ($^{11}B\{^1H\}$). Abbreviations: s = singlet, d = doublet, tr = triplet, vtr = virtual triplet, m = multiplet, n.r. = multiplet expected but not resolved, n.o. = signal not observed, pz = pyrazolide. NMR spectra were run at rt. Elemental analyses were performed by the microanalytical laboratory of the University of Frankfurt. The compounds *m*-**1**[12] and *p*-**4**[15] have been synthesized according to published procedures. For the syntheses and NMR data of *m*-**4**, *m*-**7**, *p*-**7**, and **9** see the Supporting Information of this publication.

Synthesis of *m*-5. A mixture of neat Lipz (0.50 g, 6.76 mmol) and neat Hpz (0.46 g, 6.76 mmol) was added to a stirred solution of *m*-**4** (1.15 g, 3.39 mmol) in toluene (30 mL) at rt. After the resulting suspension had been heated to reflux for 10 h, the insolubles were separated by filtration, washed with a toluene (30 mL)/hexane (20 mL) mixture, and dried *in vacuo*. Yield: 1.55 g (86%). Addition of 2 equiv of 12-crown-4 to a solution of *m*-**5** in THF (10 mL) resulted in the formation of a colorless amorphous powder. ^{11}B NMR (96.3 MHz, THF-d_8): δ 2.0 ($h_{1/2}$ = 430 Hz). ^1H NMR (300.0 MHz, THF-d_8): δ 5.99 (vtr, 4H, $^3J_{H,H}$ = 1.9 Hz, pzH-4), 6.50 (dd, 2H, $^3J_{H,H}$ = 7.3 Hz, $^4J_{H,H}$ = 1.4 Hz, H-4,6), 6.58 (m,

4H, PhH-*o*), 6.80 (tr, 1H, $^3J_{H,H}$ = 7.3 Hz, H-5), 6.92−6.99 (m, 6H, PhH-*m*,*p*), 7.31 (m, 1H, H-2), 7.38, 7.46 (2 × dd, 2 × 4H,$^3J_{H,H}$ = 2.2 Hz, 1.7 Hz, $^4J_{H,H}$ = 0.5 Hz, pzH-3,5). ^{13}C NMR (100.6 MHz, THF-d_8): δ 102.3 (pzC-4), 125.3 (PhC-*p*), 126.1 (C-5), 126.9 (PhC-*m*), 133.7 (C-4,6), 134.1 (PhC-*o*), 137.6, 139.3 (pzC-3,5), 142.4 (C-2), n.o. (CB). Anal. Calcd for $C_{30}H_{26}B_2Li_2N_8$ [534.09] × 2 $C_8H_{16}O_4$ [176.21] × 1/2 H_2O [18.02]: C, 61.70; H, 6.64; N, 12.51. Found: C, 61.71; H, 6.76; N, 12.19 (the compound is hygroscopic).

Synthesis of *p*-5. A mixture of neat Lipz (0.49 g, 6.66 mmol) and neat Hpz (0.45 g, 6.66 mmol) was added to a stirred solution of *p*-**4** (1.13 g, 3.33 mmol) in toluene (40 mL) at rt. After the resulting suspension had been heated to reflux for 18 h, the insolubles were isolated by filtration, washed with toluene (20 mL) and hexane (30 mL), and dried *in vacuo*. Yield: 1.57 g (88%). Crystals of *p*-**5**(12-c-4)$_2$ suitable for X-ray analysis were obtained by gas-phase diffusion of hexane into a saturated THF solution of *p*-**5** and 2 equiv of 12-crown-4. ^{11}B NMR (128.4 MHz, THF-d_8): δ 1.7 ($h_{1/2}$ = 380 Hz). ^{1}H NMR (400.1 MHz, THF-d_8): δ 6.06 (m, 4H, pzH-4), 6.57 (m, 4H, PhH-*o*), 6.82 (s, 4H, C_6H_4), 6.95−7.00 (m, 6H, PhH-*m*,*p*), 7.40, 7.52 (2 × d, 2 × 4H, pzH-3,5). ^{13}C NMR (62.9 MHz, THF-d_8): δ 102.4 (pzC-4), 125.3 (PhC-*p*), 126.9 (PhC-*m*), 134.0 (PhC-*o*), 134.3 (C_6H_4), 137.5, 139.4 (pzC-3,5), n.o. (CB). Anal. Calcd for $C_{30}H_{26}B_2Li_2N_8$ [534.09] × 2 $C_8H_{16}O_4$ [176.21]: C, 62.32; H, 6.59; N, 12.64. Found: C, 62.08; H, 6.71; N, 12.43.

Synthesis of *m*-8. A solution of *m*-**7** (1.60 g, 5.83 mmol) in toluene (40 mL) was added to a mixture of neat Lipz (0.86 g, 11.68 mmol) and neat Hpz (1.59 g, 23.36 mmol) at rt. After the resulting suspension had been heated to reflux for 15 h, the insolubles were collected on a frit. The colorless residue was washed with hexane (20 mL) and dried *in vacuo*. Yield: 2.28 g (76%). For further purification, the crude product was dissolved in a minimum amount of THF and precipitated into hexane. ^{11}B NMR (80.3 MHz, THF-d_8): δ 1.9 ($h_{1/2}$ = 330 Hz). ^{1}H NMR (400.1 MHz, THF-d_8): δ 6.00 (m, 6H, pzH-4), 6.37 (dd, 2H, $^3J_{H,H}$ = 7.3 Hz, $^4J_{HH}$ = 1.1 Hz, H-4,6), 6.79 (n.r., 1H, H-2), 6.87 (tr, 1H, $^3J_{H,H}$ = 7.3 Hz, H-5), 7.06, 7.45 (2 × d, 2 × 6H, $^3J_{H,H}$ = 2.0 Hz, 1.0 Hz, pzH-3,5). ^{13}C NMR (62.9 MHz, THF-d_8): δ 103.1 (pzC-4), 126.4 (C-5), 132.5 (C-4,6), 136.3, 139.8 (pzC-3,5), 140.1 (C-2), n.o. (CB). Anal. Calcd for $C_{24}H_{22}B_2Li_2N_{12}$ [514.02] × 2/3 C_4H_8O [72.11]: C, 56.98; H, 4.86; N, 29.90. Found: C, 56.47; H, 5.09; N, 29.50 (the relative amount of THF present in the sample was confirmed by ^{1}H NMR spectroscopy).

Synthesis of *p*-8. A solution of *p*-**7** (0.88 g, 3.21 mmol) in toluene (40 mL) was added to a mixture of neat Lipz (0.48 g, 6.42 mmol) and neat Hpz (0.87 g, 12.84 mmol) at rt. After the resulting suspension had been heated to reflux for 10 h, the colorless insolubles were collected on a frit, washed with toluene (20 mL), and dried *in vacuo*. Yield: 1.53 g (93%). For further purification, the crude product was dissolved in a minimum amount of THF and precipitated into hexane. ^{11}B NMR (96.3 MHz, THF-d_8): δ 2.2 ($h_{1/2}$ = 340 Hz). ^{1}H NMR (400.1 MHz, THF-d_8): δ 6.04 (dd, 6H, $^3J_{H,H}$ = 2.1 Hz, 1.7 Hz, pzH-4), 6.49 (s, 4H, C_6H_4), 7.05, 7.49 (2 × dd, 2 × 6H, $^3J_{H,H}$ = 2.1 Hz, 1.7 Hz, $^4J_{H,H}$ = 0.6 Hz, pzH-3,5). ^{13}C NMR (75.4 MHz, THF-d_8): δ 103.2 (pzC-4), 132.8 (C_6H_4), 136.3, 140.0 (pzC-3,5), n.o. (CB). Anal. Calcd for $C_{24}H_{22}B_2Li_2N_{12}$ [514.02] × 1/3 C_4H_8O [72.11] × 1 H_2O [18.02]: C, 54.72; H, 4.83; N, 30.23. Found: C, 53.88; H, 5.00; N, 29.88 (the relative amount of THF present in the sample was confirmed by ^{1}H NMR spectroscopy; the compound is hygroscopic).

Synthesis of 10. A mixture of **9** (0.71 g, 1.90 mmol), Lipz (0.42 g, 5.70 mmol), and Hpz (0.78 g, 11.40 mmol) was suspended in toluene (40 mL) and heated to reflux for 12 h. The colorless insolubles were collected on a frit, washed with toluene (50 mL), and dried *in vacuo*. Yield: 1.20 g (86%). For further purification, the crude product was washed with THF (20 mL). ^{11}B NMR (96.3 MHz, acetone-d_6): δ 2.3 ($h_{1/2}$ = 340 Hz). ^{1}H NMR (400.1 MHz, acetone-d_6): δ 5.92 (vtr, 9H, $^3J_{H,H}$ = 2.0 Hz, pzH-4), 6.45 (s, 3H, H-2,4,6), 7.12, 7.38 (d, m, 2 × 9H, $^3J_{H,H}$ = 2.0 Hz, pzH-3,5). ^{13}C NMR (62.9 MHz, acetone-d_6): δ 103.9 (pzC-4), 136.7 (pzC-3 or 5), 139.8 (C-2,4,6), 140.9 (pzC-3 or 5), n.o. (CB). Anal. Calcd for $C_{33}H_{30}B_3Li_3N_{18}$ [731.97] × 2 C_4H_8O [72.11]: C, 56.20; H, 5.29; N, 28.77. Found: C, 56.54; H, 5.05; N, 29.20 (the relative amount of THF present in the sample was confirmed by ^{1}H NMR spectroscopy).

Reaction of *m*-1 with [Mn(CO)$_5$Br]. To a solution of *m*-**1** (0.112 g, 0.20 mmol) in THF (20 mL) was added a solution of [Mn(CO)$_5$Br] (0.110 g, 0.40 mmol) in THF at rt. The reaction mixture was stirred for 16 h, whereupon a colorless precipitate formed. After filtration, the solvent was removed from the filtrate *in vacuo*. The yellow residue was recrystallized from Et_2O/hexane (2:1; 4 °C) to afford **2** as colorless crystals. Yield: 0.019 g (27%). Subsequent storage of the yellow mother liquor for a prolonged time at 4 °C resulted in the formation of yellow crystals of **3**(Et_2O). NMR data of **2**: ^{11}B NMR (128.4 MHz, THF-d_8): δ 3.0 ($h_{1/2}$ = 380 Hz). ^{1}H NMR (250.1 MHz, THF-d_8): δ 0.99 (s, 36H, CH_3), 5.98 (s, 2H, H-2), 6.17 (tr, 4H, $^3J_{H,H}$ = 2.5 Hz, pzH-4), 7.11 (tr, 2H, $^3J_{H,H}$ = 7.5 Hz, H-5), 7.45 (d, 8H, $^3J_{H,H}$ = 2.5 Hz, pzH-3,5), 7.78 (d, 4H, $^3J_{H,H}$ = 7.5 Hz, H-4,6). ^{13}C NMR (62.9 MHz, THF-d_8): δ 32.3 (CH_3), 106.6 (pzC-4), 125.7 (C-5), 131.3 (C-4,6), 138.7 (pzC-3,5), 140.2 (C-2), n.o. (CB). Anal. Calcd for $C_{40}H_{56}B_4N_8$ [692.17]: C, 69.41; H, 8.15; N, 16.18. Found: C, 69.08; H, 8.10; N, 15.88.

Reaction of *m*-5 with [Mn(CO)$_5$Br]. Neat [Mn(CO)$_5$Br] (0.47 g, 1.72 mmol) was added to a solution of *m*-**5** (0.46 g, 0.86 mmol) in THF (30 mL) at rt. After the reaction mixture had been stirred for 12 h, the solvent was removed *in vacuo*. Yellow crystals of **6**$(THF)_4$ suitable for X-ray crystallography were grown at rt by gas-phase diffusion of hexane into a THF solution of the crude product. IR (KBr, cm^{-1}): $\tilde{\nu}$(CO) 2017 (s), 1930 (s), 1904 (shoulder).

Reaction of *p*-5 with [Mn(CO)$_5$Br]. The experiment was performed similar to the reaction of *m*-**5** with [Mn(CO)$_5$Br] and also gave yellow X-ray quality crystals of **6**$(THF)_4$. Quantities: [Mn(CO)$_5$Br] (0.60 g, 2.20 mmol), *p*-**5** (0.59 g, 1.10 mmol).

Synthesis of *m*-11. [Mn(CO)$_5$Br] (0.73 g, 2.66 mmol) was dissolved in THF (20 mL) and added via syringe to neat *m*-**8** (0.68 g, 1.33 mmol). After the resulting yellow solution had been stirred for 10 h at rt, the solvent was removed *in vacuo*. CH_2Cl_2 (50 mL) was added to the colorless residue, the resulting suspension was filtered and the solvent removed from the filtrate *in vacuo* to give a yellow microcrystalline solid. Yield: 0.85 g (82%). Crystals suitable for X-ray crystallography were grown by layering a THF solution of *m*-**11** with hexane (1:2). IR (KBr, cm^{-1}): $\tilde{\nu}$(CO) 2029 (s), 1944 (s), 1922 (s). ^{11}B NMR (96.3 MHz, THF-d_8): δ 1.5 ($h_{1/2}$ = 250 Hz). ^{1}H NMR (300.0 MHz, THF-d_8): δ = 6.26 (vtr, 6H, $^3J_{H,H}$ = 2.3 Hz, pzH-4), 7.74 (m, 7H, pzH-3 or 5, H-5), 8.03 (d, 6H, $^3J_{H,H}$ = 1.8 Hz, pzH-3 or 5), 8.14 (dd, 2H, $^3J_{H,H}$ = 7.6 Hz, $^4J_{H,H}$ = 1.4 Hz, H-4,6), 8.50 (n.r., 1H, H-2). ^{13}C NMR (100.6 MHz, THF-d_8): δ 106.6 (pzC-4), 128.9 (C-5), 135.9 (C-4,6), 137.0 (pzC-3 or 5), 141.8 (C-2), 145.9 (pzC-3 or 5), n.o. (CB, CO). Anal. Calcd for $C_{30}H_{22}B_2Mn_2N_{12}O_6$ [778.09] × CH_2Cl_2 [84.93]: C, 43.14; H, 2.80; N, 19.47. Found: C, 42.94; H, 2.87; N, 19.40.

Synthesis of *p*-11. A solid mixture of *p*-**8** (0.25 g, 0.49 mmol) and [Mn(CO)$_5$Br] (0.27 g, 0.98 mmol) was dissolved in THF (30 mL) and stirred for 18 h at rt. The mixture was evaporated to dryness *in vacuo* and the yellow residue extracted into CH_2Cl_2 (2 × 30 mL). All volatiles were removed from the extract under reduced pressure to give a colorless solid. Yield: 0.27 g (71%). X-ray quality crystals were grown by gas-phase diffusion of hexane into a saturated solution of *p*-**11** in THF. IR (KBr, cm^{-1}): $\tilde{\nu}$(CO) 2025 (s), 1915 (s). ^{11}B NMR (96.3 MHz, THF-d_8): δ 1.6 ($h_{1/2}$ = 420 Hz). ^{1}H NMR (300.0 MHz, THF-d_8): δ 6.30 (n.r., 6H, pzH-4), 7.84, 8.08 (2 × n.r., 2 × 6H, pzH-3,5), 8.16 (s, 4H, C_6H_4). ^{13}C NMR (75.4 MHz, THF-d_8): δ 106.5 (pzC-4), 135.4 (C_6H_4), 137.1, 145.9 (pzC-3,5), n.o. (CB, CO). Anal. Calcd for $C_{30}H_{22}B_2Mn_2N_{12}O_6$

[778.09] × 0.25 CH_2Cl_2 [84.93]: C, 45.46; H, 2.84; N, 21.02. Found: C, 46.12; H, 3.14; N, 20.62 (the relative amount of CH_2Cl_2 present in the sample was confirmed by ^{1}H NMR spectroscopy).

Synthesis of 12. Neat [$Mn(CO)_5Br$] (0.33 g, 1.20 mmol) was added in one portion to a suspension of **10** (0.29 g, 0.40 mmol) in toluene (40 mL). The reaction mixture was stirred at rt for 12 h to give a pale yellow solution. The solvent was removed under reduced pressure and the crude product extracted into CH_2Cl_2 (2 × 40 mL). The extract was evaporated to dryness *in vacuo* to give a pale yellow microcrystalline residue. Yield: 0.42 g (92%). X-ray quality crystals were grown by gas-phase diffusion of hexane into a saturated solution of **12** in THF. IR (KBr, cm^{-1}): $\tilde{\nu}$ (CO) 2034 (s), 1931 (br). ^{11}B NMR (96.3 MHz, THF-d_8): δ −0.3 ($h_{1/2}$ = 450 Hz). ^{1}H NMR (300.0 MHz, THF-d_8): δ 6.26 (vtr, 9H, $^3J_{H,H}$ = 2.1 Hz, pzH-4), 7.82, 8.05 (2 × d, 2 × 9H, $^3J_{H,H}$ = 2.2 Hz, 1.8 Hz, pzH-3,5), 8.72 (s, 3H, H-2,4,6). ^{13}C NMR (75.4 MHz, THF-d_8): δ 106.7 (pzC-4), 136.9 (pzC-3 or 5), 141.7 (C-2,4,6), 145.9 (pzC-3 or 5), n.o. (CB, CO). Anal. Calcd for $C_{42}H_{30}B_3Mn_3N_{18}O_9$ [1128.07] × 0.5 CH_2Cl_2 [84.93] × 1 C_4H_8O [72.11]: C, 44.95; H, 3.16; N, 20.28. Found: C, 44.57; H, 3.38; N, 20.15 (the relative amount of THF and CH_2Cl_2 present in the sample was confirmed by ^{1}H NMR spectroscopy).

X-ray Crystal Structure Analysis of 2, 3(Et$_2$O), *m*-11, and 12. A single crystal of **2** was measured on a SIEMENS SMART diffractometer. Repeatedly measured reflections remained stable. An empirical absorption correction with the program SADABS[35] was performed. The structure was determined by direct methods using the program SHELXS[36] and refined against F^2 with full-matrix least-squares techniques using the program SHELXL-97.[37] All non-hydrogen atoms were refined with anisotropic thermal parameters. The hydrogen atoms at the pyrazole rings were taken from a difference Fourier synthesis and refined with individual isotropic thermal parameters. The remaining hydrogen atoms were geometrically positioned and treated as riding on the carbon atoms. The torsion angle about the C−C bond was refined for each of the six independent methyl groups.

Single crystals of **3**(Et_2O), *m*-**11**, and **12** were analyzed with a STOE IPDS II two-circle diffractometer. Empirical absorption corrections were performed using the MULABS[38] option in PLATON.[39] The structures were solved by direct methods using the program SHELXS[36] and refined against F^2 with full-matrix least-squares techniques using the program SHELXL-97.[37] All non-hydrogen atoms were refined with anisotropic displacement parameters. The hydrogen atoms were geometrically positioned and treated as riding on the carbon atoms. Compound *m*-**11** contains 1 equiv of cocrystallized CH_2Cl_2, which is disordered over two positions (occupancy factors: 0.58(1), 0.42(1)). **12** crystallizes together with 4 equiv of THF.

Acknowledgment. M.W. is grateful to the "Deutsche Forschungsgemeinschaft" (DFG). T.M. wishes to thank the "Fonds der Chemischen Industrie" (FCI) for a Ph.D. grant.

Supporting Information Available: Syntheses protocols for *m*-**4**, *m*-**7**, *p*-**7**, and **9**. Crystallographic data of **2**, **3**(Et_2O), *p*-**5**(12-c-4)$_2$, **6**$(THF)_4$, *m*-**7**, *p*-**7**, **9**, *m*-**11**, *p*-**11**, and **12** in crystallographic information file (CIF) format. This material is available free of charge via the Internet at http://pubs.acs.org. CCDC reference numbers: 689728 (**2**), 689719 (**3**(Et_2O)), 689720 (*p*-**5**(12-c-4)$_2$), 689724 (**6**$(THF)_4$), 689726 (*m*-**7**), 689723 (*p*-**7**), 689727 (**9**), 689721 (*m*-**11**), 689725 (*p*-**11**), 689722 (**12**). Structure plots and structure descriptions of *p*-**5**(12-c-4)$_2$, **6**$(THF)_4$, *m*-**7**, *p*-**7**, **9**, and *p*-**11**.

OM800504R

(35) Sheldrick, G. M. *SADABS*; University of Göttingen: Germany, 2000.
(36) Sheldrick, G. M. *Acta Crystallogr.* **1990**, *A46*, 467–473.
(37) Sheldrick, G. M. *SHELXL-97. A Program for the Refinement of Crystal Structures*; Universität Göttingen, 1997.
(38) Blessing, R. H. *Acta Crystallogr.* **1995**, *A51*, 33–38.
(39) Spek, A. L. *J. Appl. Crystallogr.* **2003**, *36*, 7–13.